BOLLETTINO DI GEOFISICA TEORICA ED APPLICATA VOL. 38, N. 3-4, pp. 165-178; SEP.-DEC. 1997

Wave dynamics at an interface between porous media

G. QUIROGA-GOODE and J. M. CARCIONE

Osservatorio Geofisico Sperimentale, Trieste, Italy

(Received July 5, 1995; accepted October 24, 1995)

Abstract. We investigate the scattered transients within the framework of Biot's low-frequency theory. The analysis, for a normally incident fast wave, considers open, mixed and closed boundary conditions. We found that, for non-dissipative media, the reflection coefficient of the slow wave decreases from open to closed boundary conditions as a result of energy transfer to the reflected fast wave. When the fluid viscosity is finite, static slow modes develop at the interface, regardless of its permeability. They are stronger in the open case. The transient analysis confirms that, in the closed case, the relative motion between the solid and the fluid phases vanishes at the interface. Moreover, the power flow balance reveals the existence of interference fluxes between the wave modes. In the transmission medium, the interference fluxes change polarity with frequency, and their main contribution shifts towards lower frequencies for low viscosities. These fluxes behave as a relaxation peak with the coefficient of resistance. In the case of ideal saturating fluids, it is confirmed that these fluxes do not contribute to the power balance.

1. Introduction

The acoustics of porous media are important because they find applications in a diversity of fields, such as reservoir characterization (Bourbie et al., 1987; Dutta and Ode, 1983), polymer physics (Johnson, 1982; Bacri and Salin, 1985), and material science (Allard, 1993). In particular, Biot theory (Biot, 1956, 1962) gives an appropriate description of the acoustics in porous media. Although the approach is phenomenological, the model has been confirmed by homogeneization theory (Auriault et al., 1985).

As is well known, Biot theory predicts the propagation of two compressional waves, a fast mode (similar to the conventional P-wave of single-phase media) and a slow mode, whose velocity is, in general, lower than the shear wave velocity. In this work, we investigate the transient

Corresponding author: J. M. Carcione; Osservatorio Geofisico Sperimentale, P.O. Box 2011, 34016 Trieste, Italy; tel. +39 40 2140345; fax +39 40 327307; e-mail: jcarcione@ogs.trieste.it

response of waves normally incident at an interface between different porous media, for different types of boundary conditions. These can be classified into open (OBC), mixed (MBC) and closed (CBC) (Deresiewicz and Skalak, 1963). In the first case, the pores of both media are completely connected, while in the third case the pores are disconnected (sealed interface). In the mixed case, the pores are partially connected, so that the boundary equations are parametrized by a surface impedance that quantifies the amount of flow across the interface.

To our knowledge, the first to compute reflection and transmission coefficients for normal incidence were Geertsma and Smit (1961). They showed that fast wave energy is dissipated by conversion to the slow wave. A similar analysis was performed by Deresiewicz and Rice (1964) for the three types of boundary conditions. Rosenbaum (1974) computed the Green's function for the open and closed conditions at an interface separating a fluid from a porous solid. More recently, Turgut and Yamamoto (1988) computed normal incidence seismograms in a stack of layers (considering open boundary conditions) and showed that, in the transmission process, some of the P-wave energy is dissipated by mode conversion to the slow mode.

In this work, we perform a detailed investigation of the wave processes occurring at and near an interface between two dissimilar porous media. We consider a fast incident compressional wave, in the presence of both a viscous and an inviscid fluid, and focus our attention on the behaviour of the slow wave. In previous articles, Carcione and Quiroga-Goode (1995, 1996) showed that the amount of fast and slow compressional energy depends on the type of source. They computed synthetic seismograms for a homogeneous medium, and showed that, in the viscous case, a static slow mode is generated at the source location. The amplitude of this mode exceeds that of the compressional wave when the source is a fluid volume injection. Here, we compute the transient response to analyze the characteristics of this static mode at the interface, for different boundary conditions and material properties.

The paper is organized as follows: the second section presents the field equations. The third section gives Green's function for a given homogeneous unbounded medium and different types of source. Then, we compute the reflection and transmission coefficients for OBC, MBC and CBC (Section 4). In Section 5 we compute the Green's function and, finally, Section 6 presents the results of some numerical simulations.

2. Field equations

The dynamic equations describing wave propagation in heterogeneous porous media are given by Biot (1962). By taking the solid rigidity equal to zero, we only model dilatational deformations, i.e., the compressional waves. The 1-D velocity-pressure formulation of Biot's (low-frequency range) poroacoustic equations, in the x-direction, is

$$\partial_t v = \beta_{11}\partial_x p + \beta_{12}\partial_x p_f + \frac{\eta}{\kappa}\beta_{12} q, \tag{1}$$

$$\partial_t q = -\beta_{21}\partial_x p - \beta_{22}\partial_x p_f - \frac{\eta}{\kappa}\beta_{22} q, \tag{2}$$

$$\partial_t p = -H\partial_x v - C\partial_x q + \dot{s}, \tag{3}$$

$$\partial_t p_f = -C\partial_x v - M\partial_x q + \dot{s}_f, \tag{4}$$

where v and q are the solid and fluid (relative to the solid) particle velocities, p is the bulk hydrostatic stress, and p_f is the fluid pressure. Here

$$H = \left[K_m^{-1} - K_s^{-1} - \phi\left(K_s^{-1} - K_f^{-1}\right)\right]K^{-1}, \tag{5}$$

$$C = \left(K_m^{-1} - K_s^{-1}\right)K^{-1}, \tag{6}$$

$$M = K_m^{-1}\,K^{-1}, \tag{7}$$

with

$$K = \phi\,K_m^{-1}\left(K_f^{-1} - K_s^{-1}\right) + K_s^{-1}\left(K_m^{-1} - K_s^{-1}\right), \tag{8}$$

where K_s, K_m and K_f are the moduli of the solid, matrix and fluid, respectively, and is the effective porosity. Moreover, η is the dynamic fluid viscosity and κ is the global permeability. Finally,

$$\mathbf{B} \equiv \begin{bmatrix} \beta_{11} & \beta_{12} \\ \beta_{21} & \beta_{22} \end{bmatrix} = \left(\rho_f^2 - \rho m\right)^{-1} \begin{bmatrix} m & -\rho_f \\ \rho_f & -\rho \end{bmatrix}, \tag{9}$$

where $\rho=(1-\phi)\,\rho_s+\phi\,\rho_f$ is the composite density, with ρ_s and ρ_f the solid and fluid densities; and $m=\alpha\rho_f/\phi$, with α the tortuosity, a dimensionless parameter that depends on the pore geometry.

The source terms s and s_f can be expressed as

$$\mathbf{S} \equiv \left(s, s_f\right)^{\mathrm{T}} = (1, \alpha)^{\mathrm{T}}\, h(t)\,\delta\left(x + x_0\right),$$

where $h(t)$ is the time history, $-x_0$ is the location ($x_0>0$) and δ denotes Dirac's delta function. In Carcione and Quiroga-Goode (1996), three cases are considered:

- Bulk source: this case assumes that the energy is partitioned between the two phases. In this case, $\alpha=1$.
- Solid source: $\alpha = 0$.
- Fluid volume injection: $\alpha = \phi^{-1}$.

3. Green's function in a homogeneous medium

The frequency-domain Green's function for a 2-D homogeneous medium was obtained in Carcione and Quiroga-Goode (1996). The 1-D solution is a particular case and, for $x > -x_0$, is given by

$$v = \psi_1 \exp\left[i\omega\left(x + x_0\right)/V_1\right] + \psi_2 \exp\left[i\omega\left(x + x_0\right)/V_2\right], \tag{10}$$

and

$$q = \chi_1 \exp\left[i\omega(x + x_0)/V_1\right] + \chi_2 \exp\left[i\omega(x + x_0)/V_2\right], \tag{11}$$

where ω is the angular frequency, and

$$V_{1(2)}^2 = \frac{2\det\mathbf{M}}{U \pm \left(U^2 - 4\det\mathbf{M}\det\mathbf{B}^{-1}\right)^{1/2}} \tag{12}$$

$$U = 2\rho_f C - \rho M - H\left(m - \frac{i}{\omega}\frac{\eta}{\kappa}\right)$$

define the complex velocities V_1 and V_2 of the fast (+sign) and slow (-sign) compressional waves. In Eq. (12)

$$\mathbf{M} = \begin{bmatrix} -H & C \\ -C & M \end{bmatrix} \tag{13}$$

Moreover, in Eqs. (10) and (11),

$$\psi_1 = \frac{(V_1V_2)^2}{V_2^2 - V_1^2}\left[\left(d_{11} - V_2^{-2}\right)s_1' + d_{12}s_2'\right], \tag{14}$$

$$\psi_2 = s_1' - \psi_1, \tag{15}$$

$$\chi_1 = -\frac{(V_1V_2)^2}{V_2^2 - V_1^2}\left[\left(d_{22} - V_2^{-2}\right)s_2' + d_{21}s_1'\right], \tag{16}$$

$$\chi_2 = s_2' - \chi_1, \tag{17}$$

where

$$\mathbf{D} \equiv \begin{bmatrix} d_{11} & d_{12} \\ d_{21} & d_{22} \end{bmatrix} = (\mathbf{BM})^{-1}, \tag{18}$$

and

$$\mathbf{S}' = \left[s_1', s_2'\right]^{\mathrm{T}} = -\frac{i\omega}{2}\mathbf{M}^{-1}\mathbf{S}, \tag{19}$$

4. Reflection and transmission coefficients

Let us consider two 1-D (inviscid) (η=0) porous media in contact at $x = 0$, and assume that a fast compressional wave, generated at $x = -x_o$ impinges upon an interface. In the incidence medium, the incident and reflected fields are

$$v_I = \exp\left[i\omega\left(x + x_0\right)/V_1\right], \tag{20}$$

$$q_I = \beta_1 \exp\left[i\omega\left(x + x_0\right)/V_1\right], \tag{21}$$

and

$$v_R = R_{11}\exp\left(-i\omega x/V_1\right) + R_{12}\exp\left(-i\omega x/V_2\right), \tag{22}$$

$$q_R = \beta_1 R_{11}\exp\left(-i\omega x/V_1\right) + \beta_2 R_{12}\exp\left(-i\omega x/V_2\right), \tag{23}$$

with

$$\beta_1 \equiv \frac{\chi_1}{\psi_1} = \frac{V_2^{-2} - d_{22}}{d_{12}}, \qquad \beta_2 \equiv \frac{\chi_2}{\psi_2} = \frac{V_1^{-2} - d_{22}}{d_{12}}, \tag{24}$$

where the characteristic equation $(d_{11}-V_i^2)\,(d_{22}-V_i^2) - d_{12}\,d_{21} = 0$, i=1, 2 has been used. On the other hand, the transmitted field is

$$v' = T_{11}\exp\left(i\omega x/V_1'\right) + T_{12}\exp\left(i\omega x/V_2'\right), \tag{25}$$

$$q' = \beta_1' T_{11}\exp\left(i\omega x/V_1'\right) + \beta_2 T_{12}\exp\left(i\omega x/V_2'\right). \tag{26}$$

Parameters R_{11} and R_{12} are the, as yet unknown, reflection coefficients of the fast and slow waves in the solid phase, and T_{11} and T_{12} are the corresponding transmission coefficients. The first subindex indicates the type of incident wave and the second denotes the scattered wave. The primed quantities correspond to the transmission medium. For simplicity, the factor exp (-$i\omega t$) has been omitted in Eqs. (20)-(26).

The boundary conditions (at x = 0) were given by Deresiewicz and Skalak (1963). They are

$$v = v', \quad q = q', \quad p = p', \quad p_f - p_f' = kq, \tag{27}$$

where k is the coefficient of resistance, also called the surface flow impedance (Rosenbaum, 1974). The inverse of k has the dimension of hydraulic permeability per unit length (Bourbie et al., 1987). Eqs. (27) model the different types of boundary conditions through the parameter k:

- k = 0 implies OBC (open interface).
- $k = \infty$ implies CBC (sealed interface). In this case, the last equation in (27) is replaced by q = 0.
- $0 < k < \infty$ implies MBC (partially open interface).

Substituting Eqs. (20)-(26) into the OBC and MBC boundary conditions gives

$$\begin{bmatrix} 1 & 1 & -1 & -1 \\ \beta_1 & \beta_2 & -\beta_1' & -\beta_2' \\ a_1 & a_2 & a_1' & a_2' \\ b_1 & b_2 & b_1' - \beta_1' k & b_2' - \beta_2' k \end{bmatrix} \begin{bmatrix} R_{11} \\ R_{12} \\ T_{11} \\ T_{12} \end{bmatrix} = \begin{bmatrix} -1 \\ -\beta_1 \\ a_1 \\ b_1 \end{bmatrix} \exp\left(i\omega x_0/V_1\right) \tag{28}$$

Similarly, CBC implies

$$\begin{bmatrix} 1 & 1 & -1 & -1 \\ \beta_1 & \beta_2 & -\beta_1' & -\beta_2' \\ a_1 & a_2 & a_1' & a_2' \\ 0 & 0 & \beta_1' & \beta_2' \end{bmatrix} \begin{bmatrix} R_{11} \\ R_{12} \\ T_{11} \\ T_{12} \end{bmatrix} = \begin{bmatrix} -1 \\ -\beta_1 \\ a_1 \\ 0 \end{bmatrix} \exp\left(i\omega x_0 / V_1\right) \tag{29}$$

Repeating the calculation for a slow compressional incident wave, we obtain for OBC and MBC:

$$\begin{bmatrix} 1 & 1 & -1 & -1 \\ \beta_1 & \beta_2 & -\beta_1' & -\beta_2' \\ a_1 & a_2 & a_1' & a_2' \\ b_1 & b_2 & b_1' - \beta_1' k & b_2' - \beta_2' k \end{bmatrix} \begin{bmatrix} R_{21} \\ R_{22} \\ T_{21} \\ T_{22} \end{bmatrix} = \gamma_s \begin{bmatrix} -1 \\ -\beta_2 \\ V_2^{-1} a_2 \\ V_2^{-1} b_2 \end{bmatrix} \exp\left(i\omega x_0 / V_2\right) \tag{30}$$

Similarly, CBC implies

$$\begin{bmatrix} 1 & 1 & -1 & -1 \\ \beta_1 & \beta_2 & -\beta_1' & -\beta_2' \\ a_1 & a_2 & a_1' & a_2' \\ 0 & 0 & \beta_1' & \beta_2' \end{bmatrix} \begin{bmatrix} R_{21} \\ R_{22} \\ T_{21} \\ T_{22} \end{bmatrix} = \gamma_s \begin{bmatrix} -1 \\ -\beta_2 \\ V_2^{-1} a_2 \\ 0 \end{bmatrix} \exp\left(i\omega x_0 / V_2\right) \tag{31}$$

where

$$a_r = -\left(H + C\beta_r\right) / V_r, \qquad b_r = -\left(C + M\beta_r\right) / V_r, \qquad r = 1,2, \tag{32}$$

and

$$\gamma_s = \frac{\psi_2}{\psi_1}. \tag{33}$$

For $\eta \neq 0$ we get the reflection and transmission coefficients by applying the correspondence principle (Biot, 1956). It can be shown that the solution can be obtained by substituting $V_r\,(\eta = 0)$ by $V_r\,(\eta \neq 0)$, where V_r, $r = 1, 2$ is given in Eq. (12).

5. Energy flow and interaction of waves

The mean energy flux is continuous across a welded interface separating two single-phase media. This is a consequence of the boundary conditions that impose continuity of stresses and particle velocities. Here, we require the continuity of the sum of the mean fluxes corresponding to each phase. This is:

$$\langle P\rangle = \mathrm{Re}\left\{-\frac{1}{2}\left[(1-\phi)p_s v^* + \phi\, p_f v_f^*\right]\right\}, \tag{34}$$

where p_s is the solid pressure, v_f is the fluid particle velocity, and Re denotes the real part. Eq. (34) is the time average power flow density over a cycle of forced oscillations, where the quantity in braces is the scalar part of the complex Poynting vector. This complex notation for computing time averages can be found, for instance, in Auld (1990).

Since $p = (1 - \phi)\, p_s + \phi\, p_f$, and $q = \phi\,(v_f - v)$, the power flow (34) can be written as

$$\langle P\rangle = \mathrm{Re}\left[-\frac{1}{2}\left(pv^* + p_f q^*\right)\right]. \tag{35}$$

which is that found in Deresiewicz and Skalak (1963).

The bulk stress p and pressure p_f can be obtained from Eqs. (3) and (4), where the time dependence exp ($-i\omega t$) is assumed. For an incident fast wave, the mean fluxes in the incidence and transmission media are proportional to

$$\mathrm{Re}\left[\left(p_{I1} + p_{R1} + p_{R2}\right)\left(v_{I1} + v_{R1} + v_{R2}\right)^* + \left(p_{f_{I1}} + p_{f_{R1}} + p_{f_{R2}}\right)\left(q_{I1} + q_{R1} + q_{R2}\right)^*\right], \tag{36}$$

and

$$\mathrm{Re}\left[\left(p_1' + p_2'\right)\left(v_1' + v_2'\right)^* + \left(p_{f_1}' + p_{f_2}'\right)\left(q_1' + q_2'\right)^*\right], \tag{37}$$

respectively, where the subindices 1 and 2 indicate the fast and slow waves. At the interface, the continuity of the mean energy flux yields

$$\langle P_I\rangle + \langle P_{R1}\rangle + \langle P_{R2}\rangle + \langle P_{I,R1}\rangle + \langle P_{I,R2}\rangle + \langle P_{R1,R2}\rangle = \langle P_1'\rangle + \langle P_2'\rangle + \langle P_{12}'\rangle, \tag{38}$$

where the primed fluxes correspond to those in the transmission medium. For instance,

$$\langle P_{R1}\rangle = -\frac{1}{2}\mathrm{Re}\left(p_{R1} v_{R1}^* + p_{f_{R1}} q_{R1}^*\right) \tag{39}$$

is the mean energy flux associated with the reflected fast wave, and

$$\langle P_{12}'\rangle = -\frac{1}{2}\mathrm{Re}\left(p_1' v_2'^* + p_2' v_1'^* + p_{f1}' q_2'^* + p_{f2}' q_1'^*\right) \tag{40}$$

is the mean energy flux associated with the interference between the transmitted fast and slow waves. When $\eta = 0$, it can be shown that this term and the sum of the last three terms in the l.h.s. of Eq. (38) vanish.

We define the following energy reflection and transmission coefficients:

$$ER_{11} = \frac{\langle P_{R1}\rangle}{\langle P_I\rangle}, \quad ER_{12} = \frac{\langle P_{R2}\rangle}{\langle P_I\rangle}, \quad ET_{11} = \frac{\langle P_1'\rangle}{\langle P_I\rangle}, \quad ET_{12} = \frac{\langle P_2'\rangle}{\langle P_I\rangle}. \tag{41}$$

For instance, when $\eta_1=\eta_2=0$, the balance is

$$1+ER_{11}+ER_{12}=ET_{11}+ET_{12}, \tag{42}$$

since the interference terms vanish.

6. Green's function for two media in contact

The Green's function can be expressed as a linear combination of the fast and slow incident and scattered waves. The Green's function corresponding to the solid particle velocity is

$$\begin{aligned} G_v(x,\omega) = &\left\{\exp\left[i\omega(x+x_0)/V_1\right]+\gamma_s\exp\left[i\omega(x+x_0)/V_2\right]\right. \\ &+(R_{11}+R_{21})\exp(-i\omega x/V_1)+(R_{12}+R_{22})\exp(-i\omega x/V_2)\Big\}H(-x) \\ &+\left\{(T_{11}+T_{21})\exp(-i\omega x/V_1')+(T_{12}+T_{22})\exp(-i\omega x/V_2')\right\}H(x) \end{aligned} \tag{43}$$

where H is the step function. The Green's function corresponding to the relative fluid particle velocity is

$$\begin{aligned} G_q(x,\omega) = &\left\{\beta_1\exp\left[i\omega(x+x_0)/V_1\right]+\beta_1\gamma_f\exp\left[i\omega(x+x_0)/V_2\right]\right. \\ &+\beta_1(R_{11}+R_{21})\exp(-i\omega x/V_1)+\beta_2(R_{12}+R_{22})\exp(-i\omega x/V_2)\Big\}H(-x) \\ &+\left\{\beta_1'(T_{11}+T_{21})\exp(-i\omega x/V_1')+\beta_2'(T_{12}+T_{22})\exp(-i\omega x/V_2')\right\}H(x) \end{aligned} \tag{44}$$

where

$$\gamma_f=\frac{\chi_2}{\chi_1}. \tag{45}$$

The particle velocities are obtained by multiplying the Green's function by the source spectrum and performing a Fourier transform (numerically) back to the time domain.

Table 1 - Material properties.

Medium		incidence (shale)	transmission (seandstone)	
Solid	bulk moduls, K_s	7.6	40	GPa
	density, ρ_s	2210	2500	kg/m^3
Matrix	bulk modulus, K_m	6.17	20	GPa
	porosity, ϕ	0.16	0.2	
	permeability, κ	0.01	600	mD
	tortuosity, α	2	2	
Fluid	bulk moduls, K_f	2.5	1.85	GPa
	density, ρ_f	1040	880	kg/m^3
	viscosity, η	1	264	cp

1 cp = 10^{-3} Pa s; 1 mD = 10^{-15} m^2

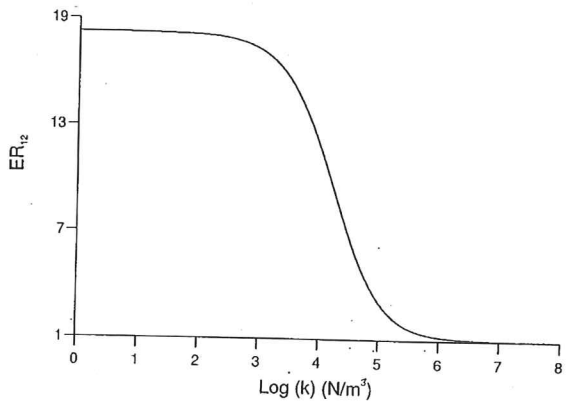

Fig. 1 - Converted energy reflection coefficient as a function of the interface resistance k for non-dissipative media.

7. Numerical examples

We consider an interface separating a brine-saturated shale (incidence medium) and an oil-saturated sandstone (transmission medium), whose material properties are given in Table 1. The low- frequency Biot theory is valid for frequencies less than $\eta\phi/(2\pi\alpha\kappa\rho_f)$, which for the media defined in Table 1 are 1220 MHz and 7.95 MHz, respectively. The time-history of the source is

$$h(t) = \sin(\omega_0 t) - \frac{1}{2}\sin(2\omega_0 t), \quad 0 < t < \frac{2\pi}{\omega_0}, \tag{46}$$

where $\omega_0 = 2\pi f_0$, with $f_0 = 4.5$ kHz the central frequency. Its time Fourier transform is

$$\tilde{h}(\omega) = \frac{-3\omega_0^3}{(\omega_0^2 - \omega^2)(4\omega_0^2 - \omega^2)}\left[\exp(2\pi i\omega / \omega_0) - 1\right]. \tag{47}$$

The distance between the source (indicated by an asterisk in the snapshots) and the interface (denoted by a vertical dotted line) is 0.75 m.

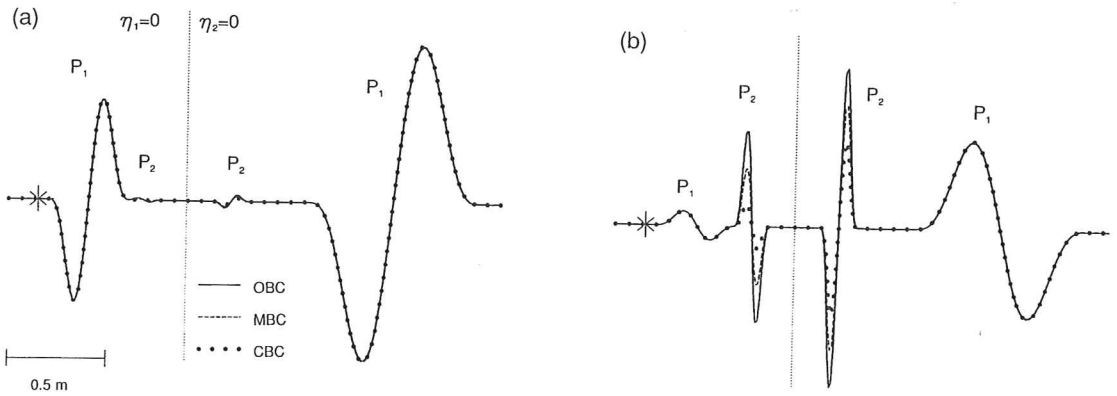

Fig. 2 - Snapshots in non-dissipative media for open, mixed and closed boundary conditions, in the center of mass particle velocity (a) and in the internal field (b), at 0.78 ms. (P_1) and (P_2) correspond to the scattered fast and slow waves, respectively.

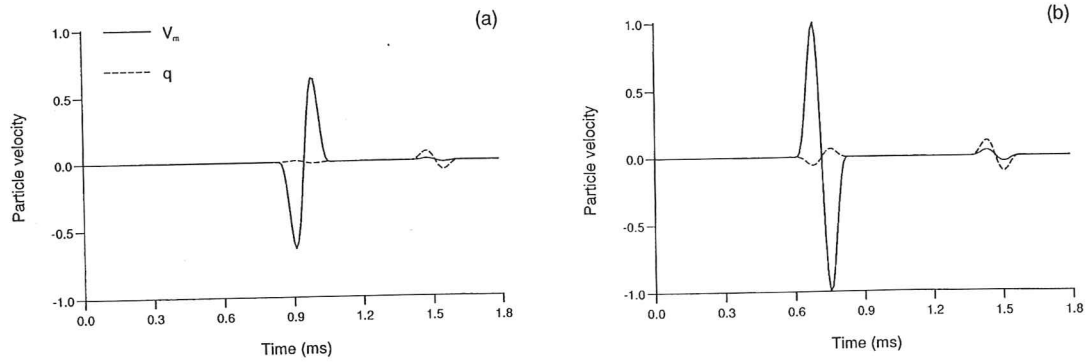

Fig. 3 - Synthetic seismograms recorded in the incidence (a) and in the transmission (b) medium of the model described in Figure 2. Receivers are located at 0.8 m from the interface.

For visualization of the wavefield we consider the "natural field variables" suggested in Sahay (1995). They are the center of mass particle velocity

$$v_m = v + \frac{\rho_f}{\rho} q \tag{48}$$

and the internal field q. In particular, v_m, the field associated with the linear momentum, is the one detected by a receiver (geophone).

Fig. 1 represents the energy reflection coefficient of the slow wave due to an incident fast wave, as a function of the coefficient or resistance k, where both media are saturated with ideal fluids ($\eta_1 = \eta_2 = 0$). The reflection coefficient is normalized with respect to the value at $k = \infty$. As stated before, $k = 0$ corresponds to open boundary conditions and $k = \infty$ to closed boundary conditions. As can be seen, the reflection coefficient decreases from OBC to CBC. This is con-

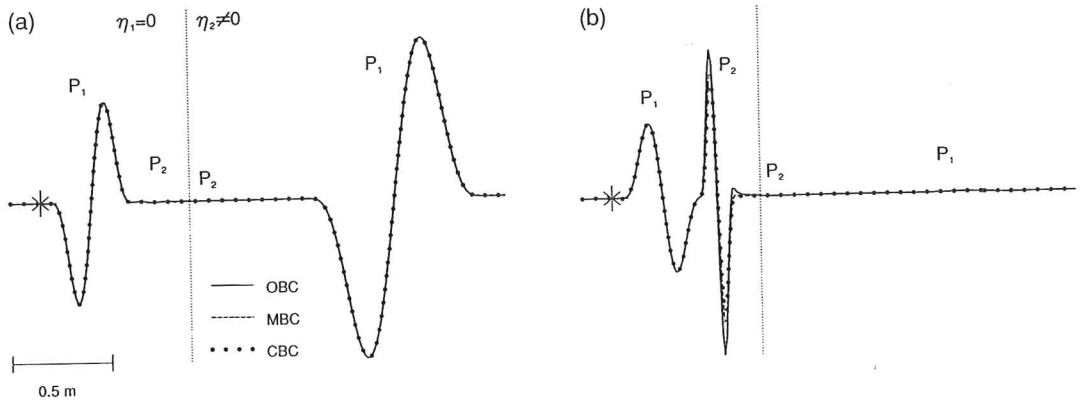

Fig. 4 - Snapshots for open, mixed and closed boundary conditions of the center of mass particle velocity (a) and the internal field (b), at 0.78 ms. Same model geometry as in Fig. 2. The converted energy in the transmission medium, permeated with a viscous fluid, has become a non-propagative mode. Note the small amplitude of the transmitted fast wave in (b).

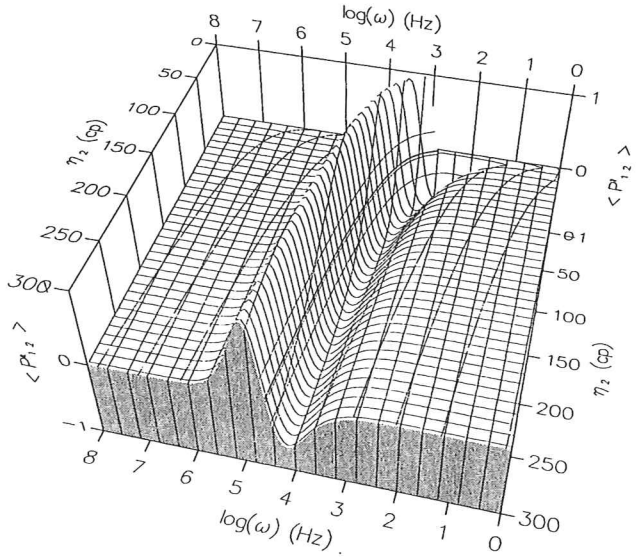

Fig. 5 - Normalized interference energy flux in the transmission medium for the model in Fig. 4 versus frequency and viscosity. Observe the shift towards the lower frequencies and viscosities, and the change in the sense of the flux with frequency.

firmed by snapshots of v_m and q represented in Figs. 2a and 2b, respectively, where the propagation time is 0.78 ms. The v_m snapshots are nearly one order of magnitude larger than the q snapshots. For a sealed interface (CBC), $q = 0$ and the reflected and transmitted slow waves decrease in amplitude with respect to the open case. It can be shown from Eq. (42) that going from OBC to CBC, the energy of the slow wave is transferred to the fast wave. In this transition, ER_{12}/ER_{11} decreases approximately by a factor of 18, qualitatively confirming the results give in Bourbie et al. (1987).

Synthetic seismograms recorded in the incidence and transmission media are displayed in Figs. 3a and 3b, respectively, where the distance between the receivers and the interface is 0.8 m. They correspond to the case of ideal saturating fluids whose snapshots are represented in Fig.

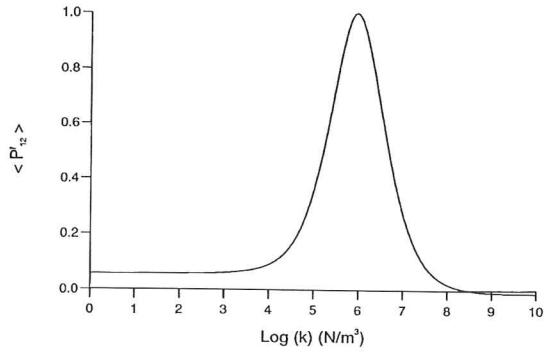

Fig. 6 - Normalized interference energy flux as a function of the coefficient of flow resistance of the interface. It corresponds to the same model as in Fig. 5.

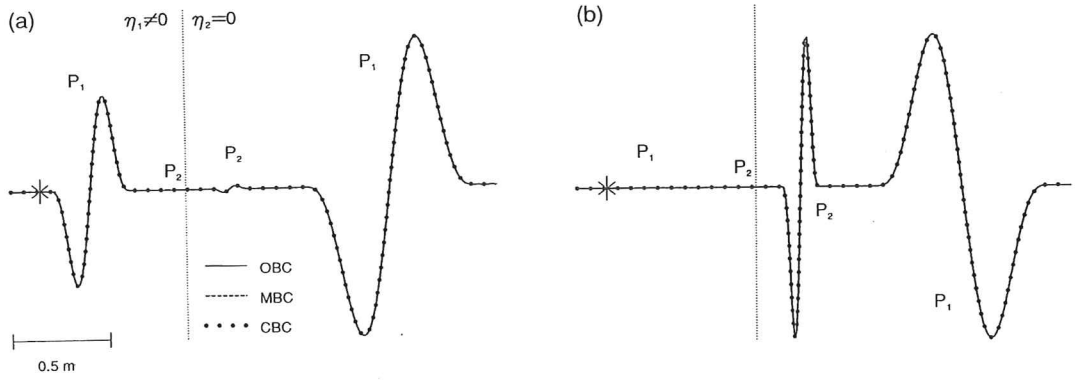

Fig. 7 - Snapshots for open, mixed and closed boundary conditions of the center of mass particle velocity (a) and the internal field (b), at 0.78 ms. The incidence and the transmission media are filled with a viscous and an inviscid saturant, respectively. In this case, as in Figure 4, the fast scattered wave is not visible in the medium permeated with a viscous fluid (in the internal field) and the converted energy has turned into a static mode.

2a (OBC).

Fig. 4 shows snapshots corresponding to $\eta_1 = 0$, $\eta_2 \neq 0$. An enlargement of the zone near the interface in the transmission medium would depict a static mode, since the slow wave is diffusive when $\eta \neq 0$. The changes in the interface permeability are mostly seen in the slow waves, as in the non-dissipative case in Fig. 2.

The interference fluxes are zero in isotropic elastic media, but they contribute to the power flow balance when the medium is viscoelastic. For instance, let us analyse the behaviour of the transmitted interference flux $\langle P'_{12} \rangle$ as a function of the frequency and the viscosity η_2. The 3-D surface represented in Fig. 5 is normalized with respect to the maximul absolute value of the interference flux. In this particular case, $\langle P'_{12} \rangle$ is six orders of magnitude smaller than the flux of the transmitted fast wave and three orders smaller than the flux of the transmitted slow mode. As can be appreciated in the figure, the main contribution shifts to the low frequencies for lower viscosities, similarly to the behaviour of the Biot relaxation peak. Moreover, the figure shows that the flow sense strongly depends on frequency.

A plot of $\langle P'_{12} \rangle$ (normalized) as a function of the coefficient of resistance k is represented in

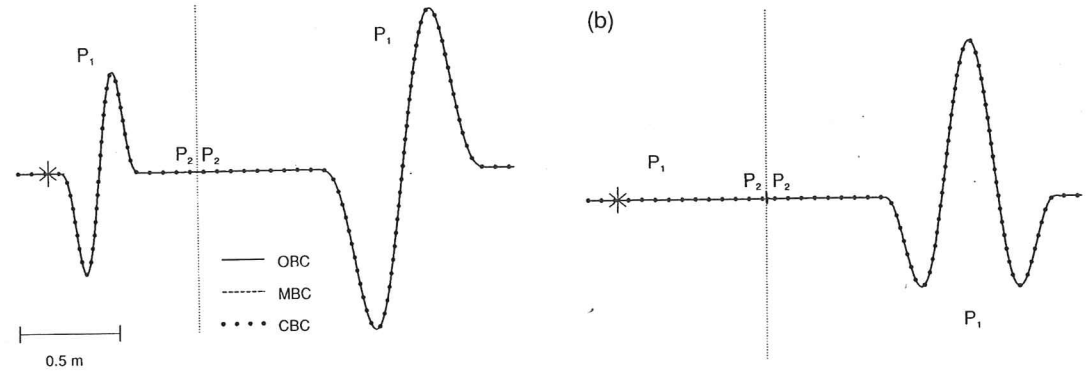

Fig. 8 - Snapshots for open, mixed and closed boundary conditions of the center of mass particle velocity (a) and the internal field (b), at 0.78 ms. The model geometry is the same as in previous Figures but both media are dissipative. Note the presence of the large amplitude static modes at both sides of the interface in (b).

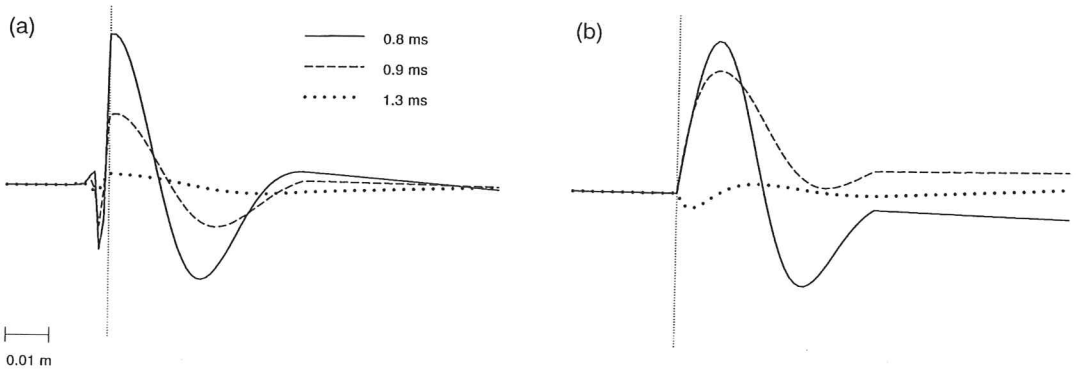

Fig. 9 - Snapshots of the internal field at different propagation times (0.8, 0.9 and 1.3 ms) in a small zone about the interface. Observe the distinct diffusive character of the static modes for open (a) and closed (b) boundary conditions. In the closed case, there is a change in polarity with propagation time and the waveforms have a similar shape as the source wavelet.

Fig. 6. The interference flux behaves as a relaxation peak, with a characteristic value k_0 for which the flux is maximum. It can be shown that for $k < k_0$, the energy is transferred to the slow mode, and that for $k > k_0$ the energy is transferred to the fast wave.

Snapshots for the cases $\eta_1 \neq 0$, $\eta_2 = 0$, and $\eta_1 \neq 0$, $\eta_2 \neq 0$, are shown in Figs. 7 and 8, respectively. In the case when the incidence medium is dissipative, the slow waves are hardly affected by the change in the coefficient of resistance, as opposed to the previous cases mentioned above. An enlargement of a small region about the interface is the dissipative case (Fig. 8) is shown in Fig. 9, where a set of snapshots of q at 0.8 ms, 0.9 ms and 1.3 ms is represented (Fig. 9a corresponds to OBC and Fig. 9b to CBC). The slow wave has a static character and shows strong dissipation with increasing time. The ratio of maximum OBC amplitude to maximum CBC amplitude for the 0.8 ms snapshot is approximately 18. Note that for CBC, $q = 0$ at the interface, in agreement with the boundary conditions (27) when $k = \infty$. In addition, there has been a polarity reversal in the snapshot at 1.3 ms.

Aknowledgements. This work was funded in part by the European Commission in the framework of the JOULE programme, sub-programme Advanced Fuel Technologies.

References

Allard J.F.; 1993: *Propagation of sound in porous media, modelling sound absorbing materials.* Elsevier Sci. Pub. Ltd., London., 284 pp.

Auld B.A.; 1990: *Acoustic fields and waves in solids.* 2 vols., R. E. Krieger Pub. Comp, 421+423 pp.

Auriault J.L., Borne L. and Chambon R.; 1985: *Dynamics of porous saturated media, checking of the generalized law of Darcy.* J. Acoust. Soc. Am., **77**, 1641-1650.

Bacri J.-C. and Salin D.; 1985: *Acoustic and hydrodynamic flows in porous media.* In Boccara N. and Daoud M., (eds), Physics of finely divided matter, Springer-Verlag Pub. Co., **5**, pp. 295-305.

Biot M.A.; 1956: *Theory of deformation of a porous viscoelastic anisotropic solid.* J. Appl. Phys., **27**, 459-467.

Biot M.A.; 1962: *Mechanics of deformation and acoustic propagation in porous media.* J. Appl. Phys., **33**, 1482-1498.

Bourbie T., Coussy O. and Zinszner B.; 1987: *Acoustic of porous media.* Institut Francais du Petrole Publ., Paris, 334 pp.

Carcione J.M. and Quiroga-Goode G.; 1995: *Some aspects of the physics and numerical modeling of Biot compressional waves.* J. Comput. Acoust., **3**, 261-280.

Carcione J.M. and Quiroga-Goode G.; 1996: *Full frequency-range transient solution for compressional waves in a fluid-saturated poroviscoacoustic medium.* Geophysical Prospecting, **44**, 99-129.

Deresiewicz H. and Skalak R.; 1963: *On uniqueness in dynamic poroelasticiy.* Bull. Seism. Soc. Am., **53**, 783-788.

Deresiewicz H. and Rice J.G.; 1964: *The effect of boundaries on wave propagation in a liquid-filled porous solid: V. Transmission across a plane interface.* Bull. Seis. Soc. Am., **54**, 409-416.

Dutta N.C. and Ode H.; 1983: *Seismic reflections from a gas-water contact.* Geophysics, **48**, 14-32.

Geertsma J. and Smit D.C.; 1961: *Some aspects of elastic wave propagation in fluid-saturated porous solids.* Geophysics, **26**, 169-181.

Johnson D.L.; 1982: *Elastodynamic of gels.* J. Chem. Phys., **77**, 1531-1539.

Rosenbaum J.H.; 1974: *Synthetic microseismograms: logging in porous formations.* Geophysics, **39**, 14-32.

Sahay P.N.; 1995: *Natural field variables in dynamic poroelasticity.* In: 64th Ann. Int. Mtg., Soc. Expl. Geophys., Expanded abstracts, pp. 1163-1166.

Turgut A. and Yamamoto T.; 1988: *Synthetic seismograms for marine sediments and determination of porosity and permeability.* Geophysics, **53**, 1056-1067.